

Phenomenology and Characterization  
of  
Spatiotemporal Chaos

--- Hitchhiker's guide to coupled map lattice world----

Kunihiko Kaneko

(金子邦彦)

Institute of Physics, College of Arts and Sciences  
University of Tokyo,  
Komaba, Meguro-ku, Tokyo 153

(東大教養物理)

Abstract

Qualitative features of coupled map lattices are presented mainly focused on the pattern competition, solitary excitations, and kink motions. Approaches for the quantitative characterizations are briefly described with the emphasis on the reconstruction problem.

S1. Introduction and Models

After the excitement of "chaos" in low dimensional dynamical systems, what has been clarified? We have understood some aspects of the onset of turbulence from the viewpoint of chaos and have also characterized weak turbulence through low dimensional chaos. Still, however, we do not know what characterizes the developed turbulence and what the essence of statistical mechanics is.

To understand the general feature of nonlinear system with a large number of degrees of freedom, we need the unification of the two aspects; i.e., the creation of local unpredictability (or local chaos) and the propagation and distribution of the local chaos among a large number of modes, which itself may occur statistically through some nonlinear mechanism. The first aspect is most easily simulated by the low-dimensional mapping system as may be phrased by the "chaos fever" a la Feigenbaum. On the other hand, we do not know so much about the second aspect. The recent studies on cellular automata are aimed to study this aspect[1]. A coupled map lattice has been proposed by some authors [2-10], mainly on the purpose of the unified study of the two aspects.

A coupled map lattice is a dynamical system with discrete time, discrete space, and continuous state[2-16]. Though there are various kinds of the above models, we restrict ourselves only to the following diffusive coupling case here[2,4,5]:

$$x_{n+1}(i) = (1-\varepsilon)f(x_n(i)) + \varepsilon/2\{f(x_n(i+1)) + f(x_n(i-1))\} \quad (1)$$

( for 1-dimensional )

or

$$x_{n+1}(i,j) = (1-\varepsilon)f(x_n(i,j)) + \varepsilon/4\{f(x_n(i+1,j)) + f(x_n(i-1,j)) + f(x_n(i,j+1)) + f(x_n(i,j-1))\} \quad (2)$$

( for 2-dimensional )

where  $n$  is a discrete time step and  $i$  ( $j$ ) is a lattice point, with the periodic boundary condition. Here the mapping function  $f(x)$  is chosen to be the logistic map

$$f(x) = 1 - ax^2,$$

(corresponding lattice is called as coupled logistic lattice (CLL1d or CLL2d)),

or the circle map

$$f(x) = x + a \sin(2\pi x) + c.$$

(the lattice is called as coupled circle lattice (CCL1d or CCL2d)).

Since some aspects have been already reported elsewhere [2,4,5,15,16], we will describe some phenomena on this system in §2,

which have not yet been reported, while some approaches on the characterization are discussed in §3.

## §2. Phenomenology

### (I) Soliton turbulence

For CCL1d, we have observed the following phase change as the parameter change:

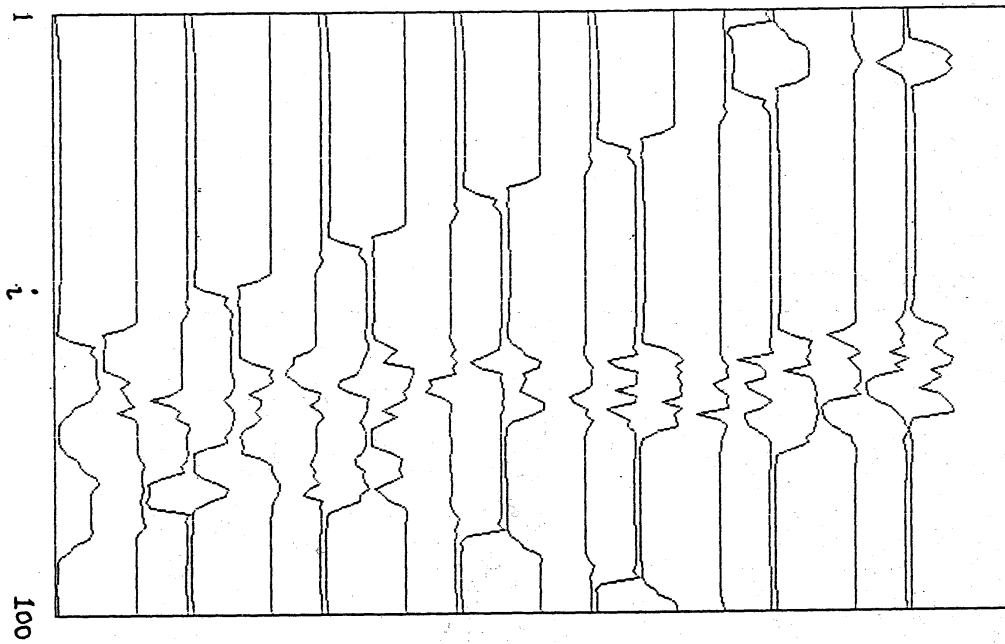
- (i) homogeneous motion
- (ii) soliton turbulence
- (iii) developed turbulence

The change (i)→(ii)→(iii) occurs as the increase of  $a$ . In Fig.1, successive patterns of CCL1d are shown while spatial derivative plots are used for some examples of CCL1d in Figs.2, i.e., the space time regions  $(i,n)$  which satisfy  $|x_n(i+1)-x_n(i)|>0.1$  are plotted as +, while the region  $|x_n(i+1)-x_n(i)|>0.05$  are plotted as ·. The pair-annihilation of kink-antikinks are clearly shown. As the increase of parameter, the collision of kink-antikinks induce the creation or annihilation of them, which cause the turbulent motion. This kind of behavior may be termed as the "soliton turbulence", in the sense that most kinks can move freely unless the collision occurs, while the sensitive dependence on the phases of the two collided kinks induce the turbulent behavior.

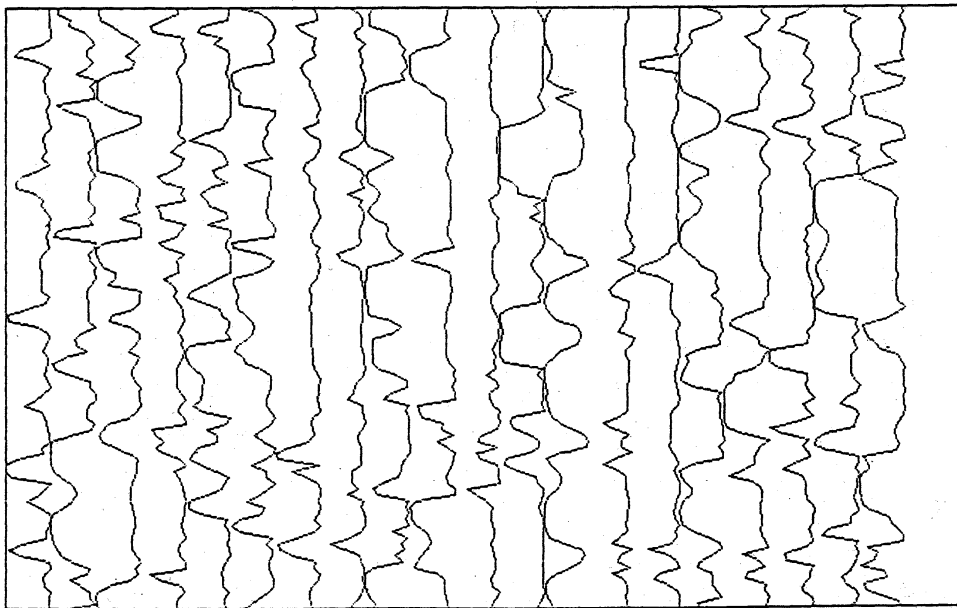
REMARK: Some investigations have been performed on the chaotic attractor on a few number of solitons, where the attractor is low-dimensional and only the soliton parameters change without the change of the number [17]. In the present case, the number itself changes chaotically. Soliton turbulence may be most easily modelled by a class of cellular automata [18,19], while Hamiltonian systems which show the soliton turbulence are investigated in [20].

As the increase of the parameter, the turbulent behavior is developed (see Fig.2c)).

For the characterization, the spatial power spectra are useful, defined by



1a)

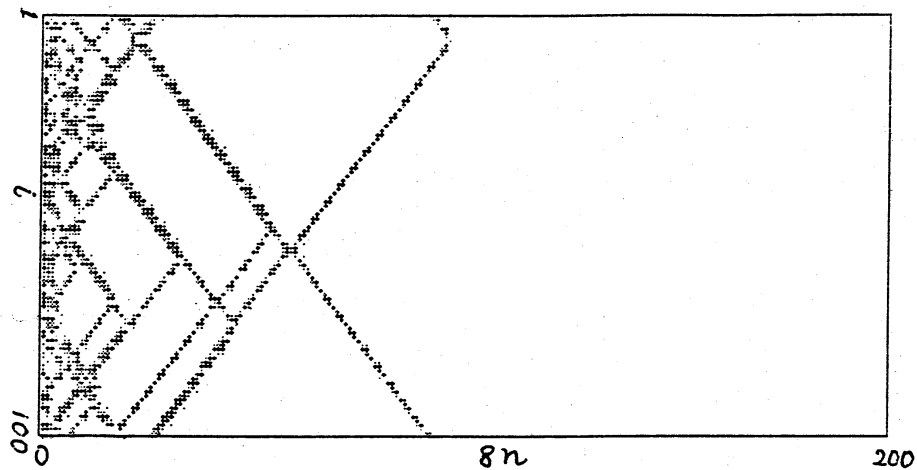


1b)

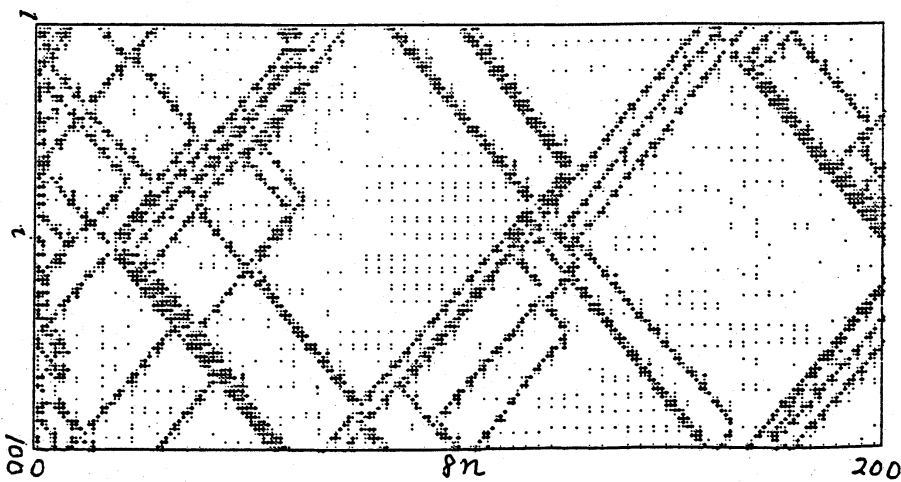
**Fig.1**  
 1a) Successive plots of  $\cos(2\pi x_n(i))$  for  $n=960+16 \cdot h$  ( $h=1,2, \dots, 20$ ). Model CCL1d;  $a=1.5$ ,  $\varepsilon=0.4$ ,  $c=0.4$ , and  $N=100$ . Random initial condition (RIC).  
 1b) Same plots for  $n=800+16 \cdot h$  ( $h=1,2, \dots, 20$ ). Model CCL1d,  $a=1.6$ ,  $\varepsilon=0.4$ ,  $c=0.4$ , and  $N=100$ . RIC.

**Fig.2 (next page)**  
 Spatial derivative plots for CCL1d with  $\varepsilon=0.2$  and  $N=100$  (see text).  
 2a)  $a=1.5$ ,  $c=0.4$  by 8 steps  
 2b)  $a=1.56$ ,  $c=0.4$  by 8 steps      2c) continued from 2b)  
 2d)  $a=1.6$ ,  $c=0.4$  by 8 steps

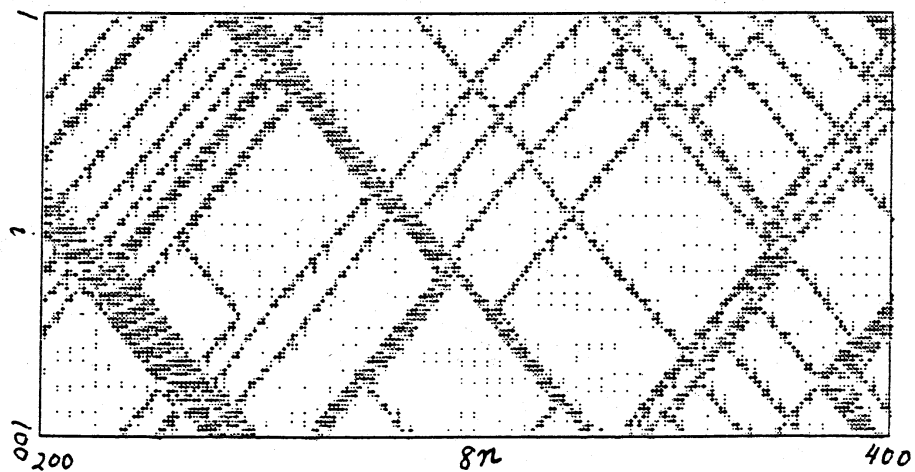
32



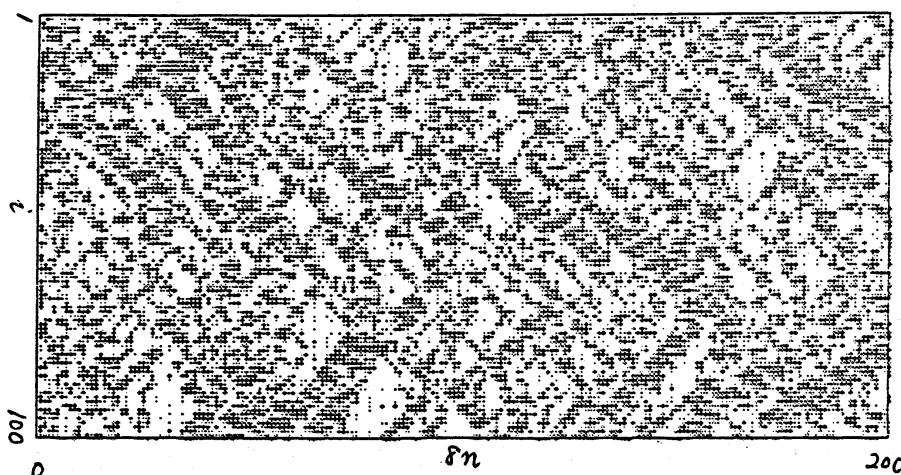
2a)



2b)



2c)



2d)

$$S(k) = \langle\langle |\sum \cos(2\pi x(j)) \exp(2\pi i k j)|^2 \rangle\rangle,$$

where  $\langle\langle***\rangle\rangle$  is the time average (for CLL we use  $x(j)$  instead of  $\cos(2\pi x(j))$ ). At the decaying kink-antikinks regions  $k^{-\alpha}$ -like behavior is observed for low-wavelength modes at the transient time regions, till finally the system falls down into a homogeneous state. As the nonlinearity is increased, we have the spectra similar to Fig. 3d). For fully developed regions, it is approximated by  $\exp(-\text{const.} \times k^2)$  [10].

#### (II) Soliton turbulence and pattern competition [15]

In a class of coupled map lattices, two patterns with  $k=0$  and  $k=k_p$  compete. That is, the powerspectra show the peaks at  $k=0$  and  $k=k_p$ . In Figs. 3 successive changes of the spatial powerspectra are shown for CLL1d with  $\varepsilon=0.3$ . At  $a=1.75$ , a peak at  $k=k_p=1/6$  is prominent. Pattern competition is clearly seen at  $a=1.8$ . As the further increase of nonlinearity, fully developed turbulence is attained (Fig. 3d)).

The local structure changes intermittently between these two elementary patterns. As has been investigated recently [15], the pattern competition induces an intermittent behavior which is characterized by the low frequency noise ( $f^{-\alpha}$ ) for the modes with  $k=k_p$ . As the parameter is changed, the following feature has been observed:

(i) The regular pattern with  $k=k_p$ :

(ii) Small chaotic embryos with  $k=0$  appear in the "sea" of the regular pattern with  $k=k_p$ , which travel in the "sea". An example of the pattern is shown in Fig. 4, where  $k_p=1/2$  and only the regions  $|x_n(i+1) - x_n(i-1)| > 0.1$  are plotted. We note the soliton-like propagation of the region with  $k=k_p$ . At  $a=1.8$ , one-way soliton-like motion finally remains after long transients (NOTE: original model is symmetric), while a kind of soliton turbulence is observed for  $a=1.85$  and  $1.9$ .

(iii) As the increase of nonlinearity  $a$ , the peak in the powerspectra at  $k=k_p$  gradually decreases till the form is fitted by  $\exp(-\text{const.} \times k^2)$ ,

34

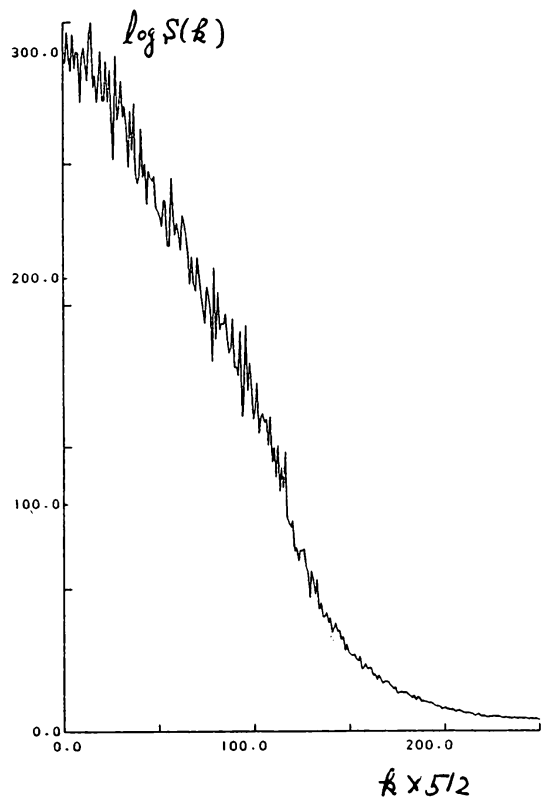
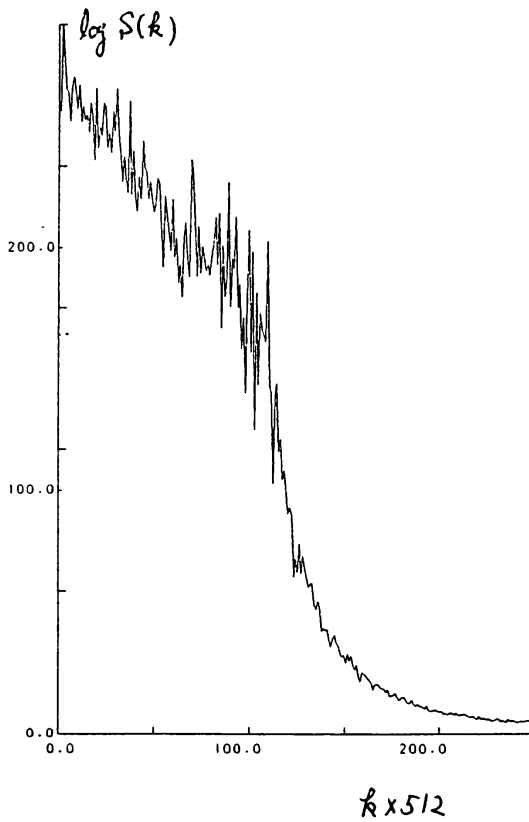
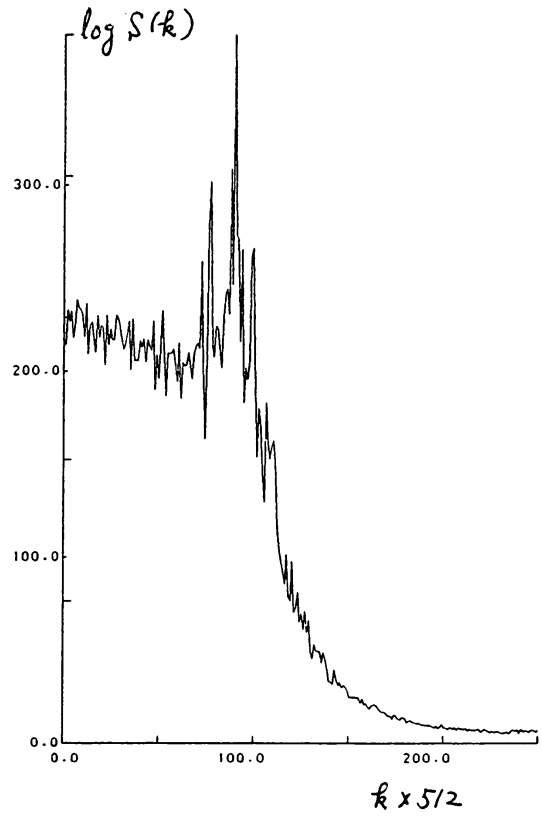
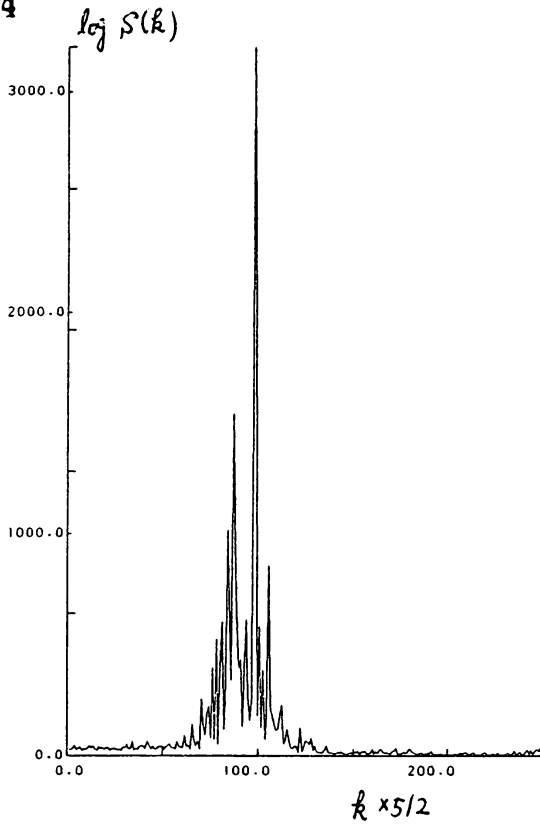
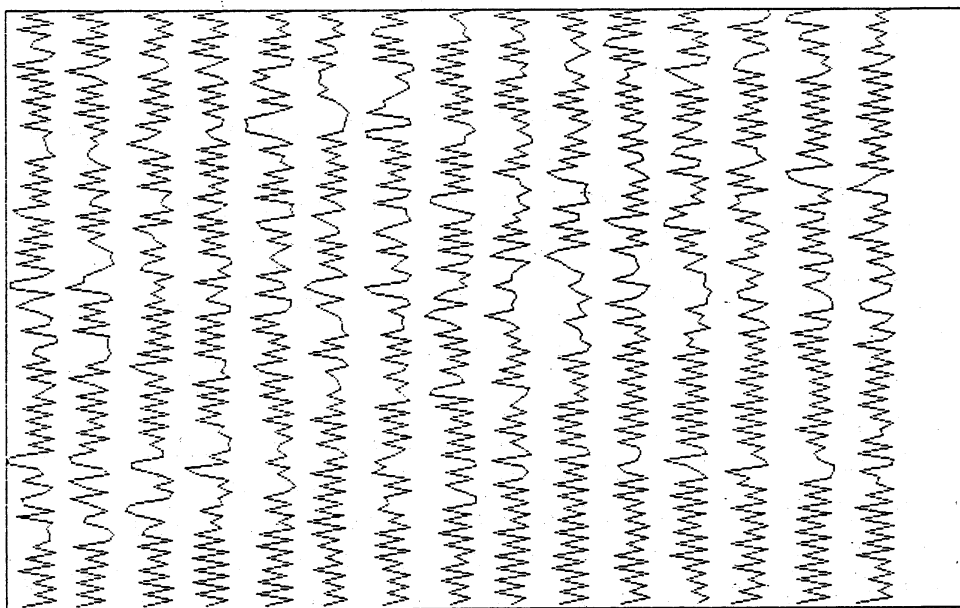
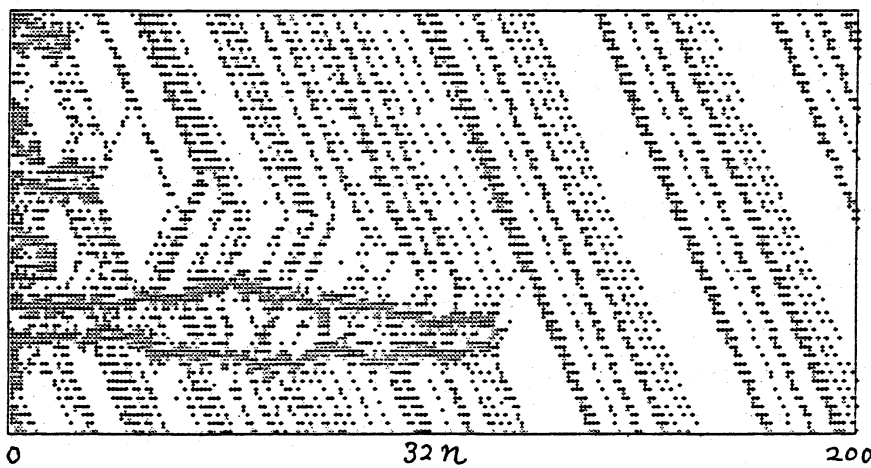


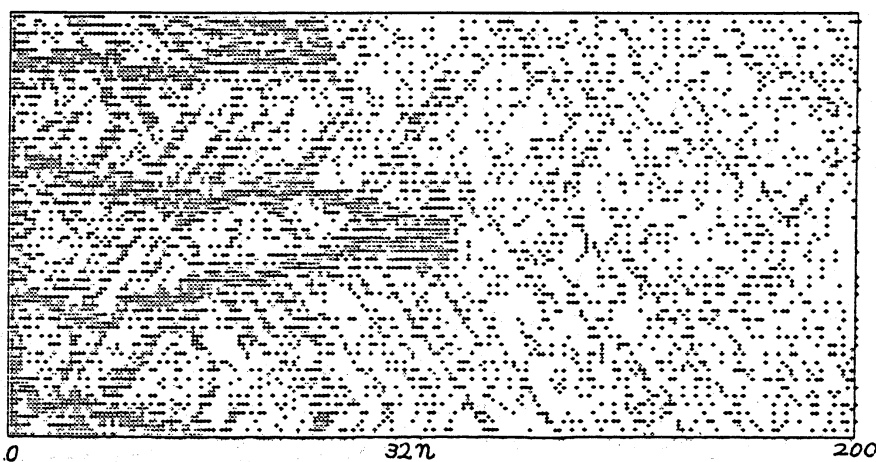
**Fig.3**  
 Spatial powerspectra  $S(k)$  for CLL1d with  $\varepsilon=0.3$ ,  $N=1024$ . RIC.  
 $\log(S(k))$  is calculated from 2000 time averages after 1000 transients.  
 3a)  $a=1.75$                       3b)  $a=1.8$   
 3c)  $a=1.85$                       3d)  $a=1.9$



4a)



4b)



4c)

Fig.4

- 4a)  $x_n(i)$ 's are plotted for  $n=800+16 \cdot h$  ( $h=1,2,\dots,15$ ). Model CLL1d;  $a=1.9$ ,  $\varepsilon=0.1$ , and  $N=100$ . Random initial condition (RIC).  
 4b) 4c) Spatial derivative plots per two sites for CLL1d ( see text)  
 4b)  $a=1.8$ ,  $\varepsilon=0.1$  by 32 steps  
 4c)  $a=1.85$ ,  $\varepsilon=0.1$  by 32 steps



which corresponds to the fully developed turbulence in our model (Fig. 3d)).

Another useful visualization for the spatiotemporal chaos is spatial Lorenz plot, where the points  $\{x_n(i), x_n(i+1)\}$  are plotted successively. Examples are shown in Figs. 5, where the pattern corresponding to  $k=k_p$  and other regions with  $k=0$  are clearly seen.

(III) Two-dimensional patterns: Chaotic motion of kinks:

In two-dimensional CMLs, the patterns show much richer behavior: kink-antikink motions, vortex-like motion, and so on. Here some examples for CCL2d are shown, where the arrows indicate the vectors  $[\cos(2\pi x_n(i)), \sin(2\pi x_n(i))]$ . The parameter here is chosen so as the single circle map shows the period-three locking with topological chaos. Thus, the homogeneous period-three motion exists. In the present parameter, some kinks which separate the different phase regions of oscillations move chaotically in time. The behavior seems to be quite similar to the domain dynamics observed in the pattern formation problems in the first order phase transitions [21]. A remarkable difference, however, lies in that the domain dynamics is not easily reduced to the curvature dynamics but is governed by deterministic chaos, since the values of  $x$  at the kink regions can show the sensitive dependence ( $|f'(x)| > 1$  as average) due to topological chaos in the single circle map. (See [22] for an oscillator lattice with random frequency.)

As a statistical mechanics problem the above phenomenon gives the following question:

Since the space without kinks are nearly homogeneous, we may expect the existence of some reduced dynamics which includes only the chaotic motion of kinks. One may expect that the reduction is performed by the choice of kink motions. In the present problem, however, the number of kinks can change. Thus the dynamical system of the kink motion must allow the change of the number of dynamic variables also. This kind of a varying dynamical system is investigated in a biological context[23], while the present case may give an example in a physical context. Construction of a concrete way of reduction and the characterization of chaos in such system is a future problem.

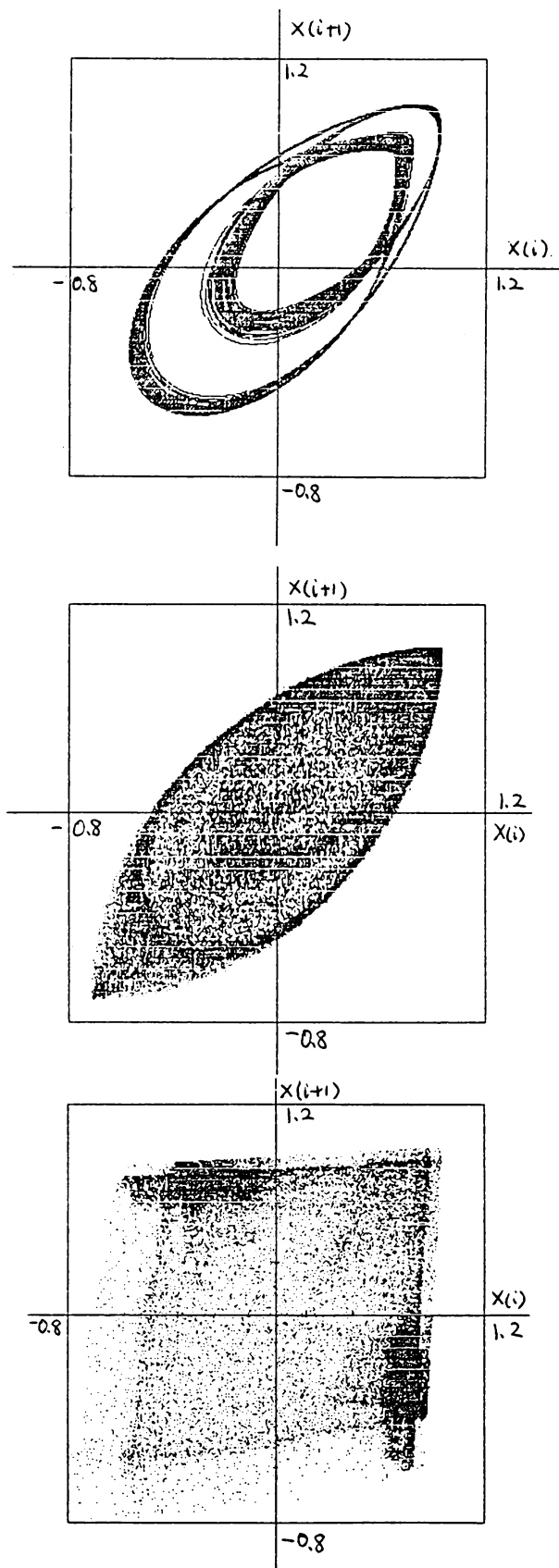
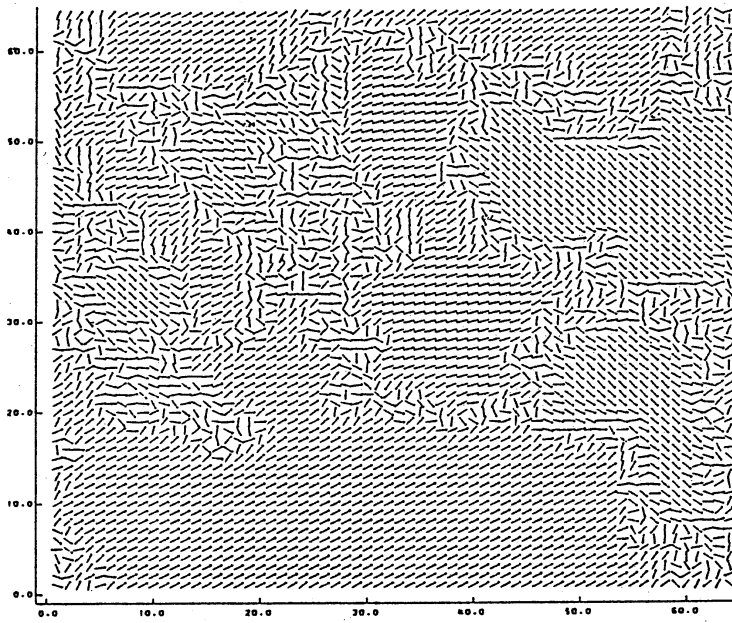
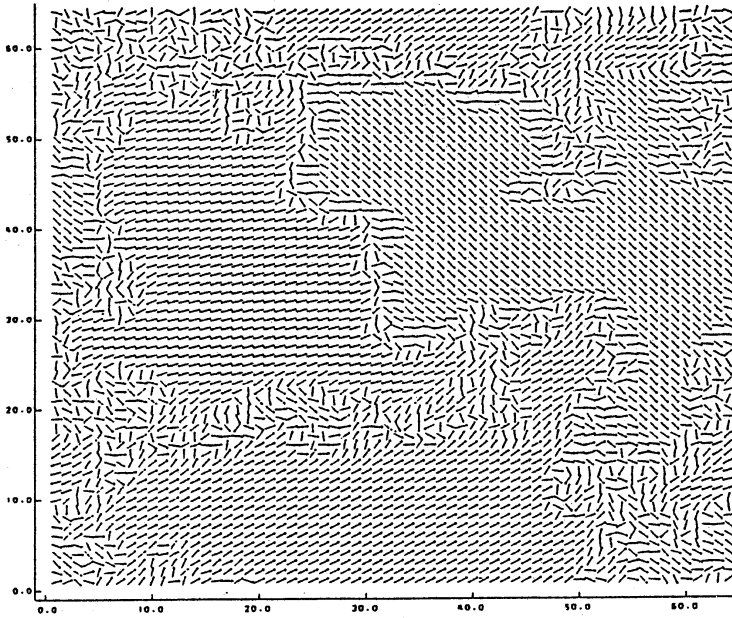


**Fig. 5**  
 Spatial Lorenz plots:  $(x_n(i), x_n(i+1))$ 's are plotted for all  $i$ .  
 $n=1000, 1001, 2000$ . CLL1d: RIC:  $N=128$   
 5a)  $a=1.75$  and  $\varepsilon=0.55$   
 5b)  $a=1.7$  and  $\varepsilon=0.5$   
 5c)  $a=1.8$  and  $\varepsilon=0.1$

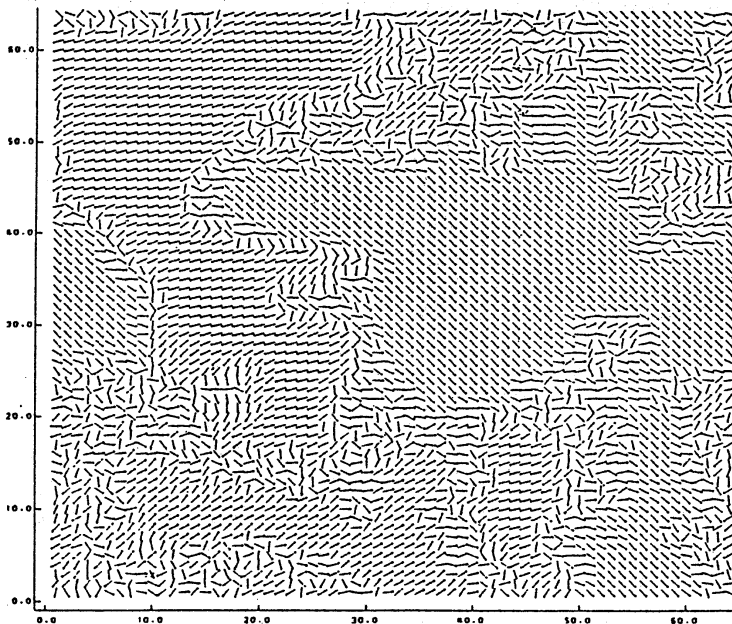
38



$n = 6000$



$n = 6180$



$n = 6360$

- Fig. 6  
Patterns of CCL2d

$a=1,2, \epsilon=0.8, c=0.37$   
64x64 lattice  
RIC

### 3. Characterization of Spatiotemporal chaos

How is the spatiotemporal chaos quantitatively characterized? Some ways have already been proposed, though we do not yet know a good and simple way of quantitative characterization. Examples of the methods are:

#### (i) Extension of dimensions

In low-dimensional systems, attempts have been performed for the reconstruction of dynamics from experimental data [24]. The algorithm commonly used is

(1) Take a time series of some variables and embed in  $k$ -dimensions i.e., construct a vector  $Z(t_i) = \{ z(t_i), z(t_i+T), \dots, z(t_i+(k-1)T) \}$ , where  $z$  is an observable and  $T$  is the sampling interval. ( following Packard et al. [25] and Takens [26] )

(2) Calculate the correlation integral  $C(r)$ , the ratio of the points in data which satisfy  $|Z(t_i) - Z(t_j)| < r$ . The scaling exponent  $d$  ( $C(r) \propto r^d$  for small  $r$ ) converges as the embedding dimension  $k$  is increased, if the data are generated by a low-dimensional dynamical system. (following Grassberger and Procaccia [27])

In our problem the attractor is high-dimensional and the above algorithm does not work. Then how can we characterize the spatiotemporal chaos?

The algorithm we have to construct is

(a) Reconstruction of local dynamics and spatial coupling term from experimental data in space-time: Though the separation of local chaos and spatial diffusion ( or flow ) may not be performed rigorously, it may be performed approximately.

(b) Estimation of the dimension density: Since the degree of relevant freedoms increase linearly as size in most spatiotemporal chaos [12], the density is a well-defined quantity.

(c) Extension of the dimensions to characterize the spatial correlation and spatial coupling.

Up to now we have not yet succeeded in the construction of the above algorithms. Here we apply the above Takens-Packard-Grassberger-Procaccia algorithm directly to our system and see what happens.

If the system size is large, the above exponent  $d$  does not converge within our possible choice of embedding dimensions ( less than  $\sim 40$  ).

Numerical simulations show the following features for fully developed turbulence.

As in Fig. 7,  $C(r)$  is well approximated by  $C(r) \propto r^{d(k)}$  for embedding dimension  $k$ . Here  $C(r)$  is calculated from a time series of  $x_n(i)$  of the model CLL1d. We note that

$$d(k) \propto k^s$$

with  $s \approx 0.6$  for the parameters in Fig.8. The exponent  $s$  changes by the choice of the parameters which scatters around 0.5-0.7 for CLL1d.

If the data were purely random,  $s$  should have taken 1. The above value of  $s$  seems to represent the diffusive nature of our model. If a small disturbance  $\delta(r)$  is applied at  $r=0$ , it is enhanced and propagates roughly as [5]

$$\delta(r,t) = \exp(\lambda t) \times \exp(-r^2 / Dt)$$

Thus the mode which affects in the embedding steps  $k$  increases as  $k^{1/2}$ , since the effective spatial regions for the time interval  $t$  increases proportionally to  $(Dt)^{1/2}$ . Our numerical results seem to give some corrections on  $s$  from the above estimate  $s=1/2$ .

If the turbulence is not yet developed, the function  $C(r)$  is not easily approximated by  $r^d$  and the slope changes by  $r$ . If the spatiotemporal chaos is composed of local chaos with separated scales (e.g. by kinks),  $C(r)$  has more than one slopes separated by flat regions. This is the case with CLL1d with weak nonlinearity.

(ii) Lyapunov spectra and Lyapunov vectors [5]:

Analogy with the Anderson localization for the vectors corresponding to the positive Lyapunov exponents have been discussed. The overlappings of Lyapunov vectors are related with the propagation of disturbances in the turbulent media.

(iii) Co-moving Lyapunov Exponents [8]:

This exponent is introduced for the study of the enhancement of a disturbance with some given speeds, which will be useful in the characterization of the spatial propagation of disturbance. Practically, the quantity is hard to measure and some other simple ways of estimation are strongly required.

(iv) Speed of the propagation of disturbance:

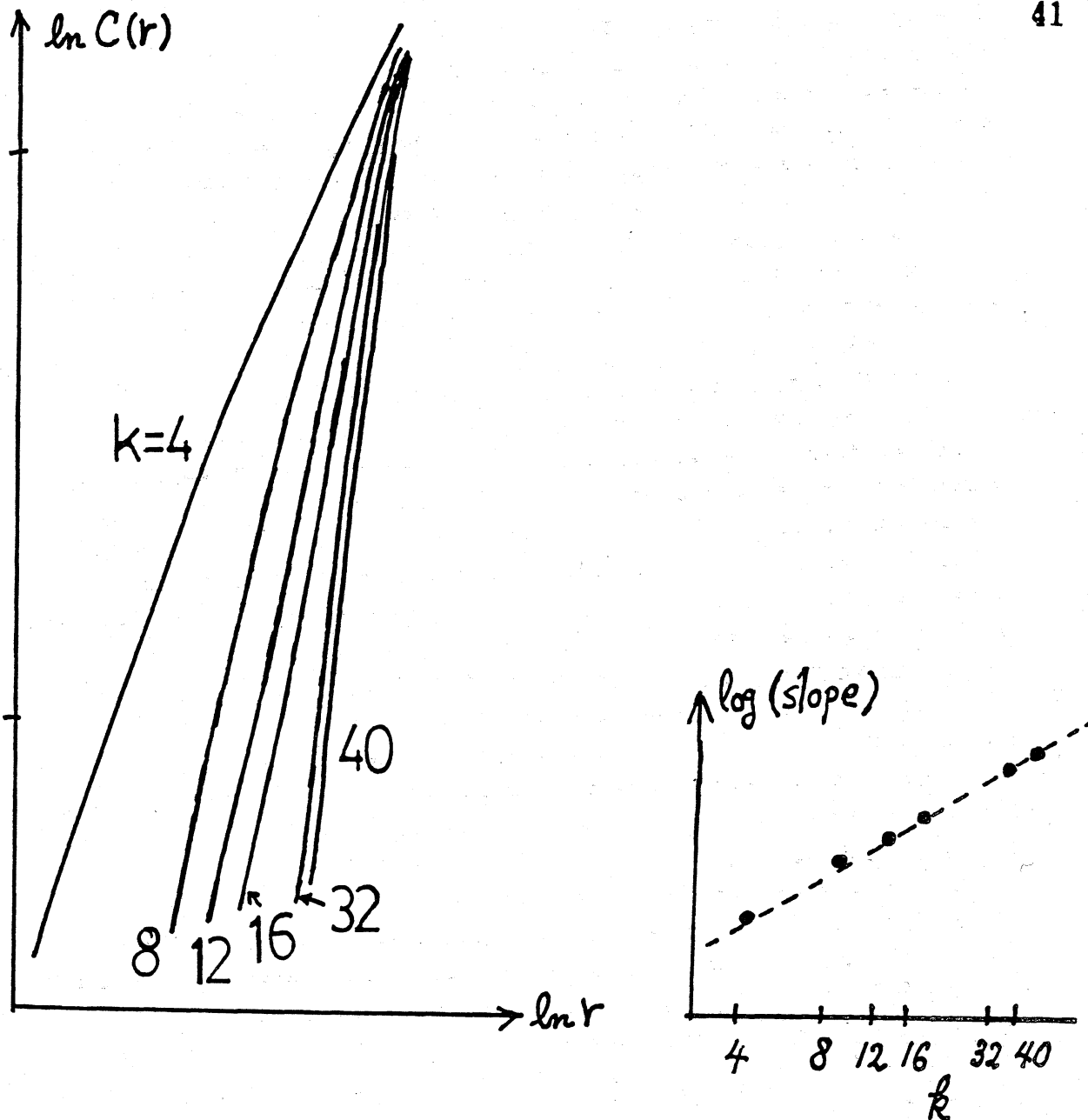


Fig.7

Log-log plots of correlation integral  $C(r)$ .  
 Model CLL1d.  $a=1.9$ ,  $\varepsilon=0.5$ , and  $N=500$ . RIC.  
 Calculated from the data at  $x(1)$  for 1000 time steps after 1000  
 transients.  
 Embedding dimensions  $k$  are 4, 8, 12, 16, 32, and 40.  
 The slope of  $\ln C(r)$  increases roughly as  $k^s$  with  $s=0.6$  as in the  
 right Figure.

The speed is obtained from the difference patterns, which can be related with Lyapunov analysis [5].

(v) Symbolic Dynamics and Entropies:

The extensions of the notions of entropies and symbolic dynamics are quite straightforward. Though we have not yet obtained any new features from these calculations, a kind of statistical mechanics formulation may be possible from this direction.

(vi) Spatial entropies and spatial Lorenz plots:

Complexity of spatial sequence is calculated for one-dimensional lattice case with the use of entropies. For the visualization, spatial Lorenz plots are useful as was shown in §2.

(vii) Spatial derivative plot and its distribution:

For the visualization of inhomogeneous regions, spatial derivative plots are introduced as was seen in §2. For the quantitative characterization, the distribution function of spatial derivative plots are useful, i.e.,

$P(y)\delta y =$  Ratio of the points s.t.  $y < |x(i+1)-x(i)| < y+\delta y$ , from which we can, for example, estimate the density of some specified patterns such as kinks.

(viii) Power spectra and correlation functions:

They are commonly used in nonlinear dynamics. In the spatio-temporal chaos, both the time and spatial transformations are useful. As is used in the pattern competition problem [15], some filtering procedure can extract an intermittent nature.

(ix) Information flow [5]:

Chaotic system creates information [29]. Through the spatial coupling term, the information is distributed into other elements. For one-dimensional systems the comoving mutual information flow has been calculated, to clarify the propagation with some speed.

(x) Scaling by coarse graining

As is commonly used, coarse graining is a powerful technique in statistical physics. In the present model, we can use the coarse-graining in spacetime. An example is seen in the intermittency problem [15]. In the problem, powerspectra for some given  $k$  modes are chosen as observables. The powerspectra are calculated only within a given size  $L$  and the scaling of the low frequency modes as the size  $L$  is studied. The low-frequency spectra for the mode near  $k=k_p$  increase as

size even if suitably normalized ("superrelevant"), while those for other modes stay constant ("relevant") or decrease as  $L$  ("irrelevant"). The scaling analysis gives a new light on the spatiotemporal intermittency and will also be useful to extract a collective motion.

#### §4. Summary

In the present paper we have reported some aspects in the phenomenology of coupled map lattices and discussed some approaches of the characterization of spatiotemporal chaos. A lot of questions lie in the study of spatiotemporal chaos. Though we have not discussed here, Hamiltonian version of coupled map lattices [30] may shed a new light on the study of ergodicity, Arnold diffusion, phase space structure.

I hope the coupled map lattice approach gives us a new perspective and leads us to a new paradigm in future.

#### Acknowledgements:

I would like to thank Dr. Jim Crutchfield, Dr. S. Takesue, Mr. Yukito Iba, Dr. M. Sano and Mr. Tetsuro Konishi for enlightning discussions and critical comments. I am also grateful to Institute of Plasma Physics at Nagoya for the facility of FACOM M-200 and VP-200.

#### References

- 1) See e.g., Theory and Applications of Cellular Automata (ed. S. Wolfram, World Sci. Pub. Co., 1986)
- 2) K. Kaneko, Ph. D. Thesis "Collapse of Tori and Genesis of Chaos in Dissipative systems" (1983); World Sci. Pub. (1986)
- 3) J. Crutchfield, Dr. Thesis (Univ. of California, 1983)
- 4) K. Kaneko, Prog. Theor. Phys. 72 (1984) 480; 74 (1985) 1033
- 5) K. Kaneko, Physica D, in press
- 6) R. Deissler, Phys. Lett. 100A (1984) 451
- 7) K. Kaneko, Phys. Lett. 111A (1985) 321
- 8) R. Deissler and K. Kaneko, preprint (1985) (LA-UR-85-3249)



- 9) I. Waller and R. Kapral, Phys. Rev. 30A (1984) 2047  
R. Kapral, Phys. Rev. 31A (1985) 3868
- 10) T. Yamada and H. Fujisaka, Prog. Theor. Phys.72 (1985) 885
- 11) J. D. Keeler and J. D. Farmer, to appear in Physica D
- 12) J. Crutchfield and K. Kaneko, in preparation ( extensive review on spatiotemporal chaos)
- 13) F. Kaspar and H.G. Schuster, Phys. Lett. 113A (1986) 451
- 14) T. Bohr et al., preprint(1986)
- 15) K. Kaneko "Intermittency by Pattern Competition and Coarse Grained Analysis for Filtered Power Spectra" in preparation
- 16) K. Kaneko , in the proceeding of US-Japan Statistical Plasma Physics(1986, IPP-report, Nagoya) and in preparation
- 17) K. Nozaki and N. Bekki, in Dynamical Problems in Soliton Systems (ed. S. Takeno, Springer, 1985)
- 18) K. Kaneko in 1)
- 19) Y. Aizawa, I. Nishikawa, and K. Kaneko, in preparation
- 20) T. Konishi, in these proceedings
- 21) see e.g., K. Kawasaki, Annals of Physics 154 (1984) 319
- 22) see e.g., Y. Kuramoto, Physica 106 A (1981) 128, S. Shinomoto, preprint, H. Daido, preprint
- 23) J. D. Farmer, S. A. Kauffman and N. H. Packard, to appear in Physica 22D (1986)
- 24) Dimensions and Entropies in Chaotic Systems ( Springer, 1986, ed. G. Mayer-Kress)
- 25) N. H. Packard et al., Phys. Rev. Lett 45 (1980) 712
- 26) F. Takens, in Dynamical Systems and Turbulence, (ed. D. Rand and L. S. Young, Springer, 1981)
- 27) P. Grassberger and I. Procaccia, Physica 13D (1984) 34
- 28) See for the similar approach in the Benard convection problem, S. Sato, M. Sano, and Y. Sawada private communication
- 29) R. Shaw, Zeitschrift fur Naturforschung 36a(1983) 80
- 30) For the case of a two-coupled system, see e.g., C. Froeschle, Astron. Astrophys. 22 (1973) 431;  
K. Kaneko and R. Bagley, Phys. Lett. 110A (1985) 435